Many-photon scattering and entangling in a waveguide with a Λ-type atom

Denis Ilin[1,2,3] and Alexander V. Poshakinskiy[4]

[1]*School of Mathematical and Physical Sciences, University of Technology Sydney, Ultimo, New South Wales 2007, Australia*

[2]*Sydney Quantum Academy, Sydney, New South Wales 2000, Australia*

[3]*Department of Physics and Technology, ITMO University, St. Petersburg 197101, Russia*

[4]*ICFO-Institut de Ciencies Fotoniques, The Barcelona Institute of Science and Technology, 08860 Castelldefels (Barcelona), Spain*

(Received 2 October 2023; revised 9 November 2023; accepted 26 February 2024; published 14 March 2024)

We develop the analytical theory that describes simultaneous transmission of several photons through a waveguide coupled to a Λ-type atom. We show that after transmission of a short few-photon pulse, the final state of the atom and all the photons is a genuine multipartite entangled state belonging to the W class. The parameters of the input pulse are optimized to maximize the efficiency of three- and four-partite W-state production. The probability to obtain the canonical W state of many photons is shown to be larger than $1/e$.

DOI: 10.1103/PhysRevA.109.033710

I. INTRODUCTION

The generation of entangled states is of paramount importance for modern quantum technologies [1,2]. Two-photon entangled Bell states are the basis of quantum communication. Multipartite entanglement is harder to achieve as it requires all the particles to interact. However, it promises strong benefits, e.g., Greenberger-Horne-Zeilinger (GHZ) states can be used for superdense coding and quantum teleportation between several parties [3]. W states [4] are also suitable for these tasks [5] but, in contrast to GHZ states, their entanglement is robust against the loss of one of the particles. Multipartite entangled cluster states [6] can implement measurement-based quantum computing [7].

Polarization-entangled photons can be obtained with linear optics elements only using Knill-Laflamme-Milburn (KLM) protocol [8]. However, such schemes require postselection and usually have quite small success probability, which makes them hardly suitable for generation of multipartite entanglement. A promising way-around that avoids postselection is to use quantum objects that have strong nonlinear optical properties even at a few-photon scale. As such, waveguide quantum electrodynamic (WQED) setups with natural or artificial two-level atoms strongly coupled to waveguides [9–11] can perform, e.g., nonlinear-sign (NS) gate [12] and obtain entangled photons in single-rail encoding. A modulated system can generate entanglement for frequency-bin photonic qubits [13].

Atoms with more complicated level schemes offer more opportunities for entanglement generation. Consider a three-level Λ-type atom with two degenerate ground states, $|x\rangle$ and $|y\rangle$, and a single excited state $|e\rangle$, where the transitions between the $|x(y)\rangle$ state and the $|e\rangle$ state are induced by $X(Y)$-polarized photons (Fig. 1). Such setup enables a single-photon Raman interaction (SPRINT), a process when an X-polarized photon after scattering by the atom in the $|x\rangle$ state becomes Y-polarized and the atom switches to the $|y\rangle$ state [14,15]. This allows to realize the SWAP operation between the states of the atom and a single photon [16–18]. A multistep protocol to entangle a train of single photons was also proposed [19]. Systems with more complicated four-level schemes, e.g., a quantum dot in an external magnetic field, were demonstrated to generate linear polarization-entangled photonic clusters [20–22]. Long-lived quantum correlations of photons also arise in such system [23]. To generate two-dimensional (2D) cluster states, waveguide and cavity QED setups were proposed [24,25].

Importantly, all previous proposals for deterministic few-photon entangling were multistep protocols where certain quantum operations should be performed on the emitter between the subsequent emission of entangled photons [19,20,24,25]. Here, we show how many-photon entangled states can be generated in a single shot by a Λ-type atom in a waveguide, see Fig. 1. We consider the atom in the $|x\rangle$ state that is excited by a few-photon short X-polarized pulse. Note that upon transmission at most one of the photons can switch from X to Y polarization [15]. Indeed, after emission of the Y-polarized photon, the atom gets to the $|y\rangle$ state and does not interact with the subsequent X-polarized photons. As this conversion can happen to any one photon, the final state appears to be a polarization-entangled state of all the photons and the atom.

While the essence of the effect is quite intuitive, the calculation of the scattering matrix for more than one photon is a complicated problem. For two-level atoms, the few-photon scattering amplitude was first calculated in Ref. [26] using the Bethe ansatz. Then, the result for two photons was reproduced by several other simpler methods [27–29], and the quite general theories of many-photon scattering based on input-output formalism [30,31] and master-equation approach [32] were developed. Three-level Λ-type atoms were often exploited in schemes where only one of the transitions is coupled to waveguide photons and the other is driven by external field leading to quantum correlations in the emission [33–36]. However, to entangle photons, there must be at least two orthogonal photonic states, thus two active transitions are required. For Λ-type atoms where both transitions are coupled to waveguide photons, only the scattering of single photons [37–44], or trains of single photons with large delay [19,45],

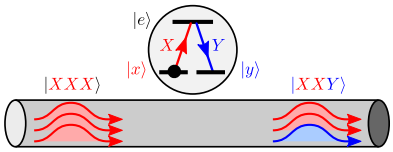

FIG. 1. Schematics of the photon transmission through a waveguide coupled to a Λ-type atom. If the atom in $|x\rangle$ state is excited by several X-polarized photons, one of them can be converted to Y polarization.

was considered up to now. Using the diagrammatic approach, we obtain simple explicit expressions for two- and three-photon scattering matrices, including the frequency-mixing terms, which allow us to maximize the efficiency of photon entangling. The generalization to larger photon numbers is straightforward.

II. MODEL

A Λ-type three-level atom coupled to a waveguide mode is described by the Hamiltonian

$$H = \sum_k \omega_k (a^\dagger_{k,x} a_{k,x} + a^\dagger_{k,y} a_{k,y}) + \varepsilon_g (b^\dagger_x b_x + b^\dagger_y b_y) + \varepsilon_e b^\dagger_e b_e + g \sum_k (a_{k,x} b^\dagger_e b_x + a_{k,y} b^\dagger_e b_y + \text{H.c.}), \quad (1)$$

where $a_{k,x(y)}$ are the bosonic operators for the photons, $b_{x(y)}$ and b_e are the fermionic operators for the electron in the atom, $\omega_k = c|k|$ is the photon dispersion that is assumed to be the same for X- and Y-polarized waveguide modes, ε_g is the energy of the ground atomic states $|x\rangle$ and $|y\rangle$, ε_e is the energy of the excited atomic state $|e\rangle$, and g is the matrix element of dipole interaction. For the sake of simplicity we focus on the chiral case, i.e., suppose that the atom interacts with the photons moving in the waveguide in one direction only, $k > 0$. A generalization to the case of symmetric coupling is discussed in the Conclusions.

To describe photon scattering we use the diagrammatic approach outlined in Ref. [11]. First, the atomic states are dressed by interaction with the photons [Fig. 2(a)] leading to

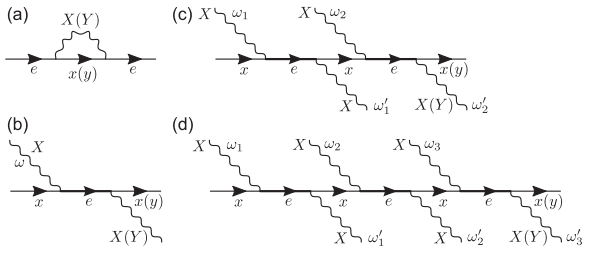

FIG. 2. Diagrammatic representation of (a) self-energy of the excited state, (b)–(d) nontrivial contributions to the transmission amplitude of one, two, and three X-polarized photons through the atom which is initially in the $|x\rangle$ state. Thin and thick solid lines denote the Green's functions of the atom in the ground state $G_{x(y)}(\varepsilon) = 1/(\varepsilon - \varepsilon_g + \text{i}0)$ and in the excited state $G_e(\varepsilon) = 1/(\varepsilon - \varepsilon_e + \text{i}\Gamma)$, respectively. Wavy lines denote photons in the waveguide, the vertices correspond to the coupling constant $g = \sqrt{c\Gamma_{1D}}$.

the imaginary correction $-\text{i}\Gamma_{1D}$ to the energy of the excited state, where $\Gamma_{1D} = g^2/c$ is the radiative decay rate of the excited state associated with the emission of a photon into the waveguide. We also introduce an additional decay rate Γ' associated with emission of a photon to the free-space modes or nonradiative decay channels. The efficiency of coupling between the waveguide and the atoms is determined by the parameter $\beta = \Gamma_{1D}/\Gamma$, where $\Gamma = \Gamma_{1D} + \Gamma'$ is the total decay rate of the excited state. Then, the photon scattering amplitudes can be calculated [Figs. 2(b) to 2(d)].

Let us briefly review the single-photon transmission [14] through the atom that is initially in the $|x\rangle$ state. Then the Y-polarized photon does not interact with the atom while the transmission of X-polarized photon is described by the diagram Fig. 2(b). The final state of the system reads $t(\omega)|Xx\rangle + s(\omega)|Yy\rangle$, which is a polarization-entangled state of the atom and the photon. Here we introduce the coefficients of photon transmission with and without polarization conversion

$$s(\omega) = -\frac{\text{i}\Gamma_{1D}}{\omega - \omega_0 + \text{i}\Gamma}, \quad (2)$$

$$t(\omega) = 1 + s(\omega) = \frac{\omega - \omega_0 + \text{i}\Gamma'}{\omega - \omega_0 + \text{i}\Gamma}, \quad (3)$$

where ω is the frequency of the photon and $\omega_0 = \varepsilon_e - \varepsilon_g$ is the frequency of the atomic transitions.

III. TWO-PHOTON SCATTERING

A. Two-photon scattering matrix

Now we consider atom in the $|x\rangle$ state that is excited simultaneously by two X-polarized photons with frequencies ω_1 and ω_2. The nontrivial contribution to the amplitude of the process, when both photons interact with the atom, is shown in Fig. 2(c). Additionally, the amplitudes of the processes when only one or none of the photons interacts have to be added. The scattering matrix elements corresponding to the final states $|XYy\rangle$ and $|XXx\rangle$ read

$$S^{XYy\leftarrow XXx}_{\omega_1',\omega_2'\leftarrow\omega_1,\omega_2} = (2\pi)^2 s(\omega_2')\delta(\omega_1 - \omega_1')\delta(\omega_2 - \omega_2') + \frac{2\pi\,\text{i}s(\omega_1)s(\omega_2')}{\omega_1 - \omega_1' + \text{i}0}\delta(\omega_1 + \omega_2 - \omega_1' - \omega_2') + (1 \leftrightarrow 2), \quad (4)$$

$$S^{XXx\leftarrow XXx}_{\omega_1',\omega_2'\leftarrow\omega_1,\omega_2} = S^{XYy\leftarrow XXx}_{\omega_1',\omega_2'\leftarrow\omega_1,\omega_2} + S^{XYy\leftarrow XXx}_{\omega_2',\omega_1'\leftarrow\omega_1,\omega_2} + (2\pi)^2[\delta(\omega_1 - \omega_1')\delta(\omega_2 - \omega_2') + \delta(\omega_1 - \omega_2')\delta(\omega_2 - \omega_1')]. \quad (5)$$

The probabilities that the atom will end in the $|x\rangle$ or $|y\rangle$ state are determined by the integrals over the final frequencies of $|S^{XXx\leftarrow XXx}|^2$ and $|S^{XYy\leftarrow XXx}|^2$, respectively. However, the second integral of $|S^{XYy\leftarrow XXx}|^2$ has nonintegrable singularities at $1/(\omega_{1(2)} - \omega_1')^2$. Interestingly, for $S^{XXx\leftarrow XXx}$ that singularities vanish and the integration result is finite, see Appendix A for the simplified expression for $|S^{XXx\leftarrow XXx}|^2$ that matches the well-known result for a two-level atom [27]. This mathematical observation has a clear physical meaning: When excited by monochromatic X-polarized light, the atom switches to the $|y\rangle$ state with the dominant probability. Indeed, as the light drives

the $|x\rangle \to |e\rangle$ transition only and the relaxation from $|e\rangle$ goes to both $|x\rangle$ and $|y\rangle$ states, the atom will eventually relax to the $|y\rangle$ state and stay there forever.

To avoid the above-mentioned singularity, excitation by pulses with finite duration rather than monochromatic continuous waves should be considered. The wave function of the incident state for the pulse consisting of two identical X-polarized photons reads

$$\psi^{(\mathrm{in})}_{t_1,t_2} = \varphi^{(0)}_{t_1}\varphi^{(0)}_{t_2}|XXx\rangle, \tag{6}$$

where $\varphi^{(0)}_t$ is the pulse envelope, $\int |\varphi^{(0)}_t|^2 dt = 1$. The transmitted pulse can be most conveniently obtained using the two-photon scattering matrix in the frequency-time domain given in Appendix B. The final state of the system is described by the wave function

$$\psi^{(\mathrm{out})}_{t_1,t_2} = \psi^{XXx}_{t_1,t_2}|XXx\rangle + \psi^{XYy}_{t_1,t_2}|XYy\rangle + \psi^{XYy}_{t_2,t_1}|YXy\rangle, \tag{7}$$

where

$$\begin{aligned}\psi^{XXx}_{t_1,t_2} &= \varphi^{(\tau)}_{t_1}\varphi^{(\tau)}_{t_2} - \left[\varphi^{(s)}_{t_<}\right]^2 \mathrm{e}^{-(\mathrm{i}\omega_0+\Gamma)|t_2-t_1|},\\ \psi^{XYy}_{t_1,t_2} &= \varphi^{(0)}_{t_1}\varphi^{(s)}_{t_2} + \theta_{t_2-t_1}\varphi^{(s)}_{t_1}\left[\varphi^{(s)}_{t_2} - \varphi^{(s)}_{t_1}\mathrm{e}^{-(\mathrm{i}\omega_0+\Gamma)(t_2-t_1)}\right],\end{aligned} \tag{8}$$

$t_< = \min(t_1, t_2)$, θ_t is the Heaviside step function, $\varphi^{(\tau)}_t = \varphi^{(0)}_t + \varphi^{(s)}_t$ describes transmission of the single-photon pulse and $\varphi^{(s)}_t = -\Gamma_{1\mathrm{D}}\int_{-\infty}^{t}\varphi^{(0)}_{t'}\mathrm{e}^{-(\mathrm{i}\omega_0+\Gamma)(t-t')}dt'$.The total probability of the two-photon pulse transmissions reads

$$T_2 = \iint \left[\left|\psi^{XXx}_{t_1,t_2}\right|^2 + 2\left|\psi^{XYy}_{t_1,t_2}\right|^2\right]dt_1 dt_2. \tag{9}$$

In the absence of losses, $\Gamma' = 0$, the unitarity of the scattering matrix yeilds $T = 1$, provided the incident pulse is normalized, which we also checked numerically.

As an example, we consider the incident pulse that has a Gaussian shape

$$\varphi^{(0)}_t = \frac{\sqrt{\gamma}}{\pi^{1/4}}\mathrm{e}^{-\mathrm{i}\omega t - \gamma^2 t^2/2}, \tag{10}$$

with $\omega = \omega_0$ and $\gamma = 0.5\Gamma$ that is shown in Fig. 3(a). The transmitted two-photon wave functions Eq. (8) are plotted by color in Figs. 3(b) and 3(c). The absence of losses is assumed, $\Gamma' = 0$. The probability of scattering in the state with two X-polarized photons, $|\psi_{XXx}(t_1, t_2)|^2$ [Fig. 3(b)], is significant only in the vicinity of the diagonal, $|t_1 - t_2| \lesssim 1/\Gamma$. Indeed, if the two photons scatter at larger delays, they do so independently and each process is described by the transmission coefficients Eq. (2) [15]. Note that at the central frequency of the pulse $t(\omega_0) = 0$ and $s(\omega_0) = 1$. Therefore, with dominant probability, the first photon is scattered in the Y polarization and the atom switches to the $|y\rangle$ state [14]. Then, the second photon passes the atom without interaction. Such case is described by $|\psi_{XYy}(t_1, t_2)|^2$ [Fig. 3(c)]. Its value is significant in the large region under the diagonal $t_1 - t_2 \gtrsim 1/\Gamma$, which corresponds exactly to the described order of the scattering events.

B. Tripartite entanglement

The wave function Eq. (8) describes the the polarization state of the system provided the two transmitted photons were detected at the times t_1 and t_2. According to the classification

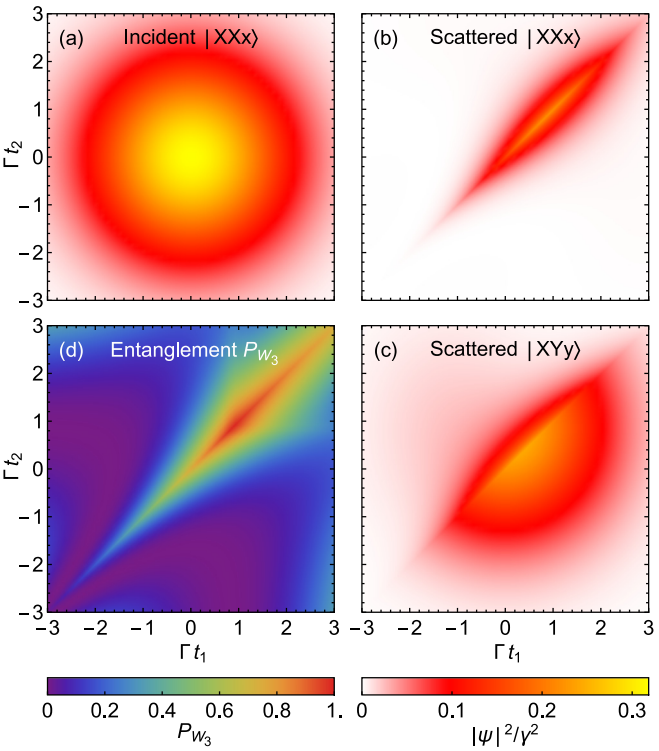

FIG. 3. Real-time wave functions of (a) the incident two-photon Gaussian pulse Eq. (10) with $\omega = \omega_0$, $\gamma = 0.5\Gamma_{1\mathrm{D}}$ and (b), (c) of the scattered pulse calculated after Eq. (8). (d) The conditional probability of converting the entangled state of the atom and two photons into the canonical W state by SLOCC given the photons are detected at times t_1 and t_2, calculated after Eq. (11). Lossless system is assumed, $\Gamma' = 0$.

of three-qubit states based on stochastic local operations and classical communication (SLOCC) [4], such a state belongs to the W class of the tripartite entanglement. Indeed, if we rename the photon polarization states $|X(Y)\rangle$ as $|0(1)\rangle$ and the atom states $|x(y)\rangle$ as $|1(0)\rangle$, the state Eq. (8) turns to be the linear combination of the states $|001\rangle$, $|010\rangle$, and $|100\rangle$, which is precisely the generalized W state.

There is no conventional measure of tripartite entanglement [1,2]. To quantify the entanglement of our state Eq. (8), we use the probability P_{W_3} with which it can be converted to the canonical W state $(|001\rangle + |010\rangle + |100\rangle)/\sqrt{3}$ by SLOCC using the procedure described in Ref. [46]. The probability is readily expressed via the coefficients of the wave function

$$P_{W_3}(t_1, t_2) = \frac{3\min\left[\left|\psi^{XXx}_{t_1,t_2}\right|^2, \left|\psi^{XYy}_{t_1,t_2}\right|^2, \left|\psi^{XYy}_{t_2,t_1}\right|^2\right]}{\left|\psi^{XXx}_{t_1,t_2}\right|^2 + \left|\psi^{XYy}_{t_1,t_2}\right|^2 + \left|\psi^{XYy}_{t_2,t_1}\right|^2}. \tag{11}$$

The color plot of $P_{W_3}(t_1, t_2)$ is shown in Fig. 3(d). The maximal values are achieved near the diagonal where all three coefficient in the wave function Eq. (7) are of the same order.

While $P_{W_3}(t_1, t_2)$ quantifies the entanglement of the atom and the photons detected at times t_1 and t_2, the total entanglement degree of the final state can be charecterized by the expected value of $P_{W_3}(t_1, t_2)$ obtained by averaging over t_1

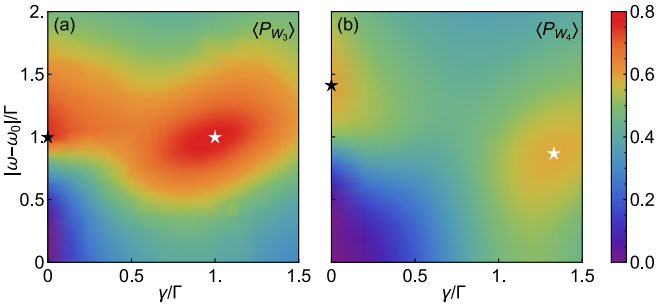

FIG. 4. (a) The expected value $\langle P_{W_3}\rangle$ of the probability of converting the final state of the atom and two photons into the canonical W state by SLOCC. The calculation is performed after Eq. (12) for the incident two-photon pulse with Gaussian envelope, Eq. (10) and no losses $\Gamma' = 0$. (b) $\langle P_{W_4}\rangle$ calculated for the three-photon pulse. Stars indicate positions of the maxima.

and t_2,

$$\langle P_{W_3}\rangle = 3\iint \min\left[\left|\psi^{XXx}_{t_1,t_2}\right|^2, \left|\psi^{XYy}_{t_1,t_2}\right|^2, \left|\psi^{XYy}_{t_2,t_1}\right|^2\right] dt_1 dt_2. \quad (12)$$

For the parameters of Fig. 3, the overlap between ψ^{XXx} and ψ^{XYy} is rather small, leading to small value of $\langle P_{W_3}\rangle$. To maximize $\langle P_{W_3}\rangle$, we tune the parameters of the incident Gaussian pulse Eq. (10). Figure 4(a) shows the color plot of $\langle P_{W_3}\rangle$ as a function of the pulse central frequency ω and the spectral width γ. The dependence is symmetric with respect to $\omega = \omega_0$ and has two maxima. The one at $|\omega - \omega_0| = \Gamma_{1D}$, $\gamma \to 0$ (black star) corresponds to the limit of a monochromatic wave. Then, the analytical calculation yields, see Appendix D,

$$\langle P_{W_3}\rangle_\omega = 3|t(\omega)|^2 \min\{|t(\omega)|^2, |s(\omega)|^2\} \quad (13)$$

that has the maximum value $\langle P_{W_3}\rangle_{\omega_0\pm\Gamma_{1D}} = 0.75$ in the absence of losses, $\Gamma' = 0$. A slightly larger value $\langle P_{W_3}\rangle \approx 0.77$ is achieved in the second maximum at $|\omega - \omega_0| \approx 0.98\Gamma_{1D}$, $\gamma \approx 0.97\Gamma_{1D}$ (white star), which corresponds to a short pulse.

IV. THREE-PHOTON SCATTERING

The above results are easily generalized for the larger number of incident photons. To show this, we consider three-photon scattering. The diagram corresponding to the nontrivial part of the process is shown in Fig. 2(d) and the three-photon scattering matrix is given by Eqs. (C1) to (C2) in the Appendix C. When there are three identical X-polarized photons in incident state, $\psi^{(\mathrm{in})}_{t_1,t_2,t_3} = \varphi^{(0)}_{t_1}\varphi^{(0)}_{t_2}\varphi^{(0)}_{t_3}|XXXx\rangle$, the final state reads

$$\begin{aligned}\psi^{(\mathrm{out})}_{t_1,t_2,t_3} &= \psi^{XXXx}_{t_1,t_2,t_3}|XXXx\rangle + \psi^{XXYy}_{t_1,t_2,t_3}|XXYy\rangle \\ &+ \psi^{XXYy}_{t_1,t_3,t_2}|XYXy\rangle + \psi^{XXYy}_{t_3,t_1,t_2}|YXXy\rangle, \end{aligned} \quad (14)$$

where

$$\begin{aligned}\psi^{XXXx}_{t_1,t_2,t_3} &= \varphi^{(\tau)}_{t_1}\varphi^{(\tau)}_{t_2}\varphi^{(\tau)}_{t_3} - \left[\varphi^{(s)}_{t_{(1)}}\right]^2\varphi^{(\tau)}_{t_{(3)}}\mathrm{e}^{-(\mathrm{i}\omega_0+\Gamma)(t_{(2)}-t_{(1)})} \\ &- \left[\varphi^{(s)}_{t_{(2)}}\right]^2\varphi^{(\tau)}_{t_{(1)}}\mathrm{e}^{-(\mathrm{i}\omega_0+\Gamma)(t_{(3)}-t_{(2)})} \\ &+ \left[\varphi^{(s)}_{t_{(1)}}\right]^2\left[\varphi^{(s)}_{t_{(2)}} - \varphi^{(0)}_{t_{(2)}}\right]\mathrm{e}^{-(\mathrm{i}\omega_0+\Gamma)(t_{(3)}-t_{(1)})}, \end{aligned} \quad (15)$$

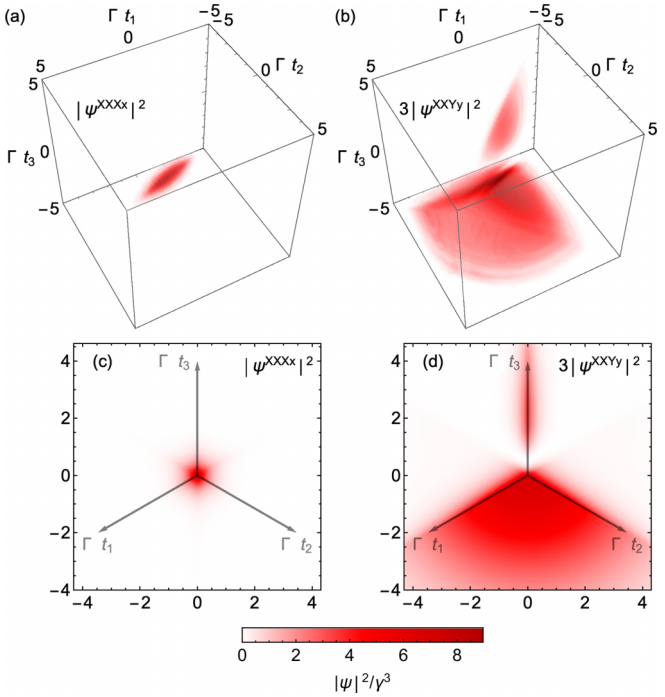

FIG. 5. (a), (b) Volume plot of the real-time wave functions of the final state for the three-photon scattering process. (c), (d) Cross section of the plots in (a,b) in the direction perpendicular to the main diagonal at $t_1 + t_2 + t_3 = 0$. Calculation is performed after Eqs. (15) to (16) for the incident three-photon pulse with Gaussian envelope, Eq. (10) with $\omega = \omega_0$, $\gamma = 0.2\Gamma$. Lossless system is assumed, $\Gamma' = 0$.

$$\begin{aligned}\psi^{XXYy}_{t_1,t_2,t_3} &= \theta_{t_<-t_3}\varphi^{(0)}_{t_<}\varphi^{(0)}_{t_>}\varphi^{(s)}_{t_3} + \theta_{t_3-t_>}\left\{\varphi^{(\tau)}_{t_<}\varphi^{(\tau)}_{t_>}\varphi^{(s)}_{t_3}\right. \\ &- \left[\varphi^{(s)}_{t_<}\right]^2\varphi^{(s)}_{t_3}\mathrm{e}^{-(\mathrm{i}\omega_0+\Gamma)(t_>-t_<)} \\ &- \left[\varphi^{(s)}_{t_>}\right]^2\varphi^{(\tau)}_{t_<}\mathrm{e}^{-(\mathrm{i}\omega_0+\Gamma)(t_3-t_>)} \\ &+ \left.\left[\varphi^{(s)}_{t_<}\right]^2\left[\varphi^{(s)}_{t_>} - \varphi^{(0)}_{t_>}\right]\mathrm{e}^{-(\mathrm{i}\omega_0+\Gamma)(t_3-t_<)}\right\} \\ &+ \theta_{t_>-t_3}\theta_{t_3-t_<}\varphi^{(0)}_{t_>}\left\{\varphi^{(\tau)}_{t_<}\varphi^{(s)}_{t_3} - \left[\varphi^{(s)}_{t_<}\right]^2\mathrm{e}^{-(\mathrm{i}\omega_0+\Gamma)(t_3-t_<)}\right\}, \end{aligned} \quad (16)$$

$t_{(1)} \leqslant t_{(2)} \leqslant t_{(3)}$ are the times t_1, t_2, t_3 sorted in the ascending order, $t_< = \min(t_1, t_2)$ and $t_> = \max(t_1, t_2)$.

Figure 5 shows $|\psi^{XXXx}_{t_1,t_2,t_3}|^2$ and $|\psi^{XXYy}_{t_1,t_2,t_3}|^2$ calculated for the Gaussian incident pulse and no losses, $\Gamma' = 0$. The probability to detect all the transmitted photons in the X polarization is nonzero only if all three detection times are close, $|t_1 - t_2|, |t_2 - t_3|, |t_3 - t_1| \lesssim 1/\Gamma$. This corresponds to the main diagonal of the coordinate frame in Fig. 5(a) and the center of the cross section shown in Fig. 5(c). Similarly to the two-photon case, that is explained by the fact that if at least one of the photons is detected with a larger delay, which means that it has scattered independently, it must convert to Y polarization since $s(\omega_0) = 1$. The probability that one of the photons is detected in Y polarization at time t_3 is shown in Figs. 5(b) and 5(d) and has a much more peculiar distribution. If the three photons are detected with large delay, it is the first of them that will be converted to Y polarization, see the region in the bottom of the cross-section Fig. 5(d) which corresponds

to $t_3 \lesssim t_1, t_2$. Alternatively, it could happen that the first two photons are transmitted simultaneously so that they keep their X polarization, which corresponds to the two-photon scattering amplitude $|\psi^{XXx}_{t_1,t_2}|^2$ depicted in Fig. 3(b). Then, the last of the three photons will be converted to Y polarization, see the line in the upper part of the cross-section Fig. 5(d) which corresponds to $t_3 \gtrsim t_1 \approx t_2$.

The entanglement of the four-partite wave function describing the final state of the atom and three photons Eq. (14) can be quantified by the probability of the conversion to the canonical four-partite W state P_{W_4} and its averaged value $\langle P_{W_4}\rangle$ which are defined in a manner similar to the three-partite case [46]

$$P_{W_4}(t_1,t_2,t_3) = \frac{4\,\mathrm{Min}\left[\left|\psi^{XXXx}_{t_1,t_2,t_3}\right|^2, \left|\psi^{XXYy}_{t_1,t_2,t_3}\right|^2, \left|\psi^{XXYy}_{t_3,t_2,t_1}\right|^2, \left|\psi^{XXYy}_{t_1,t_3,t_3}\right|^2\right]}{\left|\psi^{XXXx}_{t_1,t_2,t_3}\right|^2 + \left|\psi^{XXYy}_{t_1,t_2,t_3}\right|^2 + \left|\psi^{XXYy}_{t_3,t_2,t_1}\right|^2 + \left|\psi^{XXYy}_{t_1,t_3,t_2}\right|^2}, \tag{17}$$

$$\langle P_{W_4}\rangle = 4\iiint dt_1 dt_2 dt_3\,\mathrm{Min}\left[\left|\psi^{XXXx}_{t_1,t_2,t_3}\right|^2, \times \left|\psi^{XXYy}_{t_1,t_2,t_3}\right|^2, \left|\psi^{XXYy}_{t_3,t_2,t_1}\right|^2, \left|\psi^{XXYy}_{t_1,t_3,t_3}\right|^2\right], \tag{18}$$

where $\psi^{XXXx}_{t_1,t_2,t_3}$ and $\psi^{XXYy}_{t_1,t_2,t_3}$ are given by Eqs. (15) and (16).

Dependence of $\langle P_{W_4}\rangle$ on the parameters of the incident Gaussian pulse are shown in Fig. 4(b). As in the case of two photons, it has two maxima corresponding to monochromatic (black star) and short incident pulses (white star). In the monochromatic limit, $\gamma \to 0$, one has

$$\langle P_{W_4}\rangle_\omega = 4|t(\omega)|^4 \min\{|t(\omega)|^2, |s(\omega)|^2\}, \tag{19}$$

which reaches the maximal value $\langle P_{W_4}\rangle = 16/27 \approx 0.59$ at $|\omega - \omega_0| = \sqrt{2}\Gamma_{1D}$ for lossless case, $\Gamma' = 0$. The other maximum that corresponds to a short pulse is at $|\omega - \omega_0| \approx 0.87\Gamma_{1D}$, $\gamma \approx 1.33\Gamma_{1D}$ (white star) and gives a close value $\langle P_{W_4}\rangle \approx 0.59$.

To further improve the values of $\langle P_{W_3}\rangle$ and $\langle P_{W_4}\rangle$, the pulse shape should be optimized. By adding to the pulse higher temporal modes described by Hermite polynomials we were able to achieve $\langle P_{W_3}\rangle \approx 0.8$ and $\langle P_{W_4}\rangle \approx 0.62$, see the Appendix E for details.

One can see that the maximal value of $\langle P_{W_4}\rangle$ is smaller than that of $\langle P_{W_3}\rangle$. However, it is important to note that with the increase of the incident photon number N, the maximal value of $\langle P_{W_N}\rangle$ does not tend to zero. Instead, for any N, it remains larger than $1/e$, which is the limiting value for the quasi-monochromatic pulses, see Appendix D.

Finally, we discuss the effect of losses, $\Gamma' \neq 0$. In such a case, upon few-photon pulse transmission, some or all of the photons might be lost. Note that the remaining photons are still in the entangled state, which follows directly from the robustness of W-states against the loss of one of the particles. If the aim is to get N-photon W state without losing a photon, the probability to do so is finite, including in the $N \to \infty$ limit, and depends on the losses as $\sim\Gamma_{1D}/(\Gamma_{1D} + 2\Gamma')$, see Appendix D. Thus, the efficiency of the proposed protocol is weakly affect by loss if $\Gamma' \lesssim \Gamma_{1D}$.

V. CONCLUSION

We proposed a scheme for single-shot generation of multipartite polarization-entangled W states of a Λ-type atom and several photons in a waveguide. Given the certain robustness of the W state, the purely photonic W states can be obtained simply by disregarding the atom. We note that if the two optical transitions of the Λ atom differ in the photon propagation direction or frequency [39], then the frequency- or direction-entangled photons can be generated. While we presented the theory for the case of chiral coupling, the photon transmission in the nonchiral case is described by exactly the same equations but with the twice smaller values of $s(\omega)$ and $\varphi(s)$.

Another possible generalization is to consider an array of M Λ-type atoms excited by N-photon pulse. If initially all photons are X polarized and all atoms are in the x state, upon their interaction $0 \leqslant k \leqslant \min(N, M)$ photons can flip their polarization. Then, the final state will be the superposition of the states with k Y-polarized and $N - k$ X-polarized photons, k atoms in the y and $M - k$ atoms in the x state, with all possible k. In a chiral setup, the scattering matrix of the system is given by the product of M scattering matrices of the individual atoms, see Appendix F for this case. However, calculation of the scattering matrix for a nonchiral setup is far not straightforward and shall be the subject of future research.

For the experimental realization of the proposed protocol, the key figure of merit is the coupling factor β, which determines the probability of the photon emission into the guided mode rather than it being lost due to other decay channels. Cold atoms trapped near an optical nanofiber have still rather small efficiencies $\beta \lesssim 0.1$, see Ref. [11] for the review. High efficiencies $\beta \approx 0.99$ can be achieved in state-of-the-art setups with semiconductor quantum dots [47]. Superconducting circuits with transmon qubits [48] reach even higher values of β, but the realization of the Λ level scheme with two ground states within this platform seems challenging. A possible solution could be to use metastable states in giant-atom-like structures [49].

ACKNOWLEDGMENTS

We are grateful to A. N. Poddubny, I. V. Iorsh, and D. S. Smirnov for useful discussions. A. V. Poshakinskiy acknowledges support from the Government of Spain under Severo Ochoa Grant CEX2019-000910-S [MCIN/AEI/10.13039/501100011033], Generalitat de Catalunya (CERCA program), FundacióCellex, and Fundació Mir-Puig.

APPENDIX A: TWO-PHOTON SCATTERING BY Λ-ATOM VERSUS TWO-LEVEL ATOM

The scattering matrix element Eq. (5) after collecting all the terms is simplified to

$$S^{XXx\leftarrow XXx}_{\omega_1',\omega_2'\leftarrow\omega_1,\omega_2} = t(\omega_1)t(\omega_2)(2\pi)^2[\delta(\omega_1-\omega_1')\delta(\omega_2-\omega_2')+\delta(\omega_1-\omega_2')\delta(\omega_2-\omega_1')] + \frac{2\mathrm{i}\Gamma_{1D}^2(\omega_1+\omega_2-2\omega_0+2\mathrm{i}\Gamma)}{(\omega_1-\omega_0+\mathrm{i}\Gamma)(\omega_2-\omega_0+\mathrm{i}\Gamma)(\omega_1'-\omega_0+\mathrm{i}\Gamma)(\omega_2'-\omega_0+\mathrm{i}\Gamma)}2\pi\delta(\omega_1+\omega_2-\omega_1'-\omega_2'). \tag{A1}$$

The singularities at $\omega_{1',2'}\to\omega_{1',2'}$ that seem to be present in Eq. (5) are, in fact, canceled. Note that it is not the case for $S^{XYy\leftarrow XXx}$, Eq. (4), that is not symmetrized with respect to ω_1', ω_2' and retains the singularities.

The first line describes the coherent transmission of independent photons and the second line is the elastic two-photon scattering. The later term appears to be four times smaller than the corresponding scattering amplitude in a chiral waveguide with a two-level atom, and is exactly the same as for the two-level atom in a bidirectional waveguide [11,26,27].

APPENDIX B: TWO-PHOTON SCATTERING MATRIX IN FREQUENCY-TIME DOMAIN

We take the scattering matrix in the frequency domain Eqs. (4) and (5) and perform Fourier transform over the final frequencies ω' and ω_2'. The result is

$$\begin{aligned}S^{XXx\leftarrow XXx}_{t_1,t_2\leftarrow\omega_1,\omega_2} &= \mathrm{e}^{-\mathrm{i}\omega_1t_1-\mathrm{i}\omega_2t_2}+(\omega_1\leftrightarrow\omega_2)+s(\omega_2)\mathrm{e}^{-\mathrm{i}\omega_1t_1-\mathrm{i}\omega_2t_2}+(\omega_1\leftrightarrow\omega_2)+(t_1\leftrightarrow t_2)+(\omega_1\leftrightarrow\omega_2,t_1\leftrightarrow t_2)\\ &\quad+s(\omega_1)s(\omega_2)\theta_{t_2-t_1}\left[\mathrm{e}^{-\mathrm{i}\omega_1t_1-\mathrm{i}\omega_2t_2}-\mathrm{e}^{-\Gamma(t_2-t_1)-\mathrm{i}(\omega_1+\omega_2)t_1}\right]+(\omega_1\leftrightarrow\omega_2)+(t_1\leftrightarrow t_2)+(\omega_1\leftrightarrow\omega_2,t_1\leftrightarrow t_2)\\ &= 2\left[t(\omega_1)t(\omega_2)\cos\frac{(\omega_2-\omega_1)(t_2-t_1)}{2}-s(\omega_1)s(\omega_2)\mathrm{e}^{-(\Gamma-\mathrm{i}\frac{\omega_1+\omega_2}{2})|t_2-t_1|}\right]\mathrm{e}^{-\mathrm{i}(\omega_1+\omega_2)(t_1+t_2)/2},\end{aligned} \tag{B1}$$

$$\begin{aligned}S^{XYy\leftarrow XXx}_{t_1,t_2\leftarrow\omega_1',\omega_2'} &= s(\omega_2)\mathrm{e}^{-\mathrm{i}\omega_1t_1-\mathrm{i}\omega_2t_2}+(\omega_1\leftrightarrow\omega_2)+s(\omega_1)s(\omega_2)\theta_{t_2-t_1}\left[\mathrm{e}^{-\mathrm{i}\omega_1t_1-\mathrm{i}\omega_2t_2}-\mathrm{e}^{-\Gamma(t_2-t_1)-\mathrm{i}(\omega_1+\omega_2)t_1}\right]+(\omega_1\leftrightarrow\omega_2)\\ &= \Big\{\theta_{t_2-t_1}\Big[t(\omega_1)s(\omega_2)\mathrm{e}^{\frac{-\mathrm{i}(\omega_2-\omega_1)(t_2-t_1)}{2}}+t(\omega_2)s(\omega_1)\mathrm{e}^{\frac{\mathrm{i}(\omega_2-\omega_1)(t_2-t_1)}{2}}-2s(\omega_1)s(\omega_2)\mathrm{e}^{-(\Gamma-\mathrm{i}\frac{\omega_1+\omega_2}{2})|t_2-t_1|}\Big]\\ &\quad+\theta_{t_1-t_2}\Big[s(\omega_2')\mathrm{e}^{\frac{-\mathrm{i}(\omega_2-\omega_1)(t_2-t_1)}{2}}+s(\omega_1)\mathrm{e}^{\frac{\mathrm{i}(\omega_2-\omega_1)(t_2-t_1)}{2}}\Big]\Big\}\mathrm{e}^{-\mathrm{i}(\omega_1+\omega_2)(t_1+t_2)/2}.\end{aligned} \tag{B2}$$

APPENDIX C: THREE-PHOTON SCATTERING MATRIX

An evaluation of diagrams in Fig. 2(d) yields the three-photon scattering matrix in the frequency domain

$$\begin{aligned}S^{XXXx\leftarrow XXXx}_{\omega_1',\omega_2',\omega_3'\leftarrow\omega_1,\omega_2,\omega_3} &= \frac{-\mathrm{i}\Gamma_{1D}^3\,2\pi\delta(\omega_1'+\omega_2'+\omega_3'-\omega_1-\omega_2-\omega_3)}{(\omega_1-\omega_0+\mathrm{i}\Gamma)(\omega_1-\omega_1'+\mathrm{i}0)(\omega_1+\omega_2-\omega_1'-\omega_0+\mathrm{i}\Gamma)(\omega_3'-\omega_3+\mathrm{i}0)(\omega_3'-\omega_0+\mathrm{i}\Gamma)}\\ &\quad+\text{ [permutations of } (\omega_1',\omega_2',\omega_3') \text{ and } (\omega_1,\omega_2,\omega_3)]\\ &\quad+\frac{-\mathrm{i}\Gamma_{1D}^2\,(2\pi)^2\delta(\omega_1'+\omega_2'-\omega_1-\omega_2)\delta(\omega_3'-\omega_3)}{(\omega_1-\omega_0+\mathrm{i}\Gamma)(\omega_1-\omega_1'+\mathrm{i}0)(\omega_2'-\omega_0+\mathrm{i}\Gamma)}\\ &\quad+\text{ [permutations of } (\omega_1',\omega_2',\omega_3') \text{ and } (\omega_1,\omega_2,\omega_3)]\\ &\quad+[1+s(\omega_1')+s(\omega_2')+s(\omega_3')](2\pi)^3\delta(\omega_1'-\omega_1)\delta(\omega_2'-\omega_2)\delta(\omega_3'-\omega_3)\\ &\quad+\text{ [permutations of } (\omega_1,\omega_2,\omega_3)],\end{aligned} \tag{C1}$$

$$\begin{aligned}S^{XXYy\leftarrow XXXx}_{\omega_1',\omega_2',\omega_3'\leftarrow\omega_1,\omega_2,\omega_3} &= \frac{-\mathrm{i}\Gamma_{1D}^3\,2\pi\delta(\omega_1'+\omega_2'+\omega_3'-\omega_1-\omega_2-\omega_3)}{(\omega_1-\omega_0+\mathrm{i}\Gamma)(\omega_1-\omega_1'+\mathrm{i}0)(\omega_1+\omega_2-\omega_1'-\omega_0+\mathrm{i}\Gamma)(\omega_3'-\omega_3+\mathrm{i}0)(\omega_3'-\omega_0+\mathrm{i}\Gamma)}\\ &\quad+\text{ [permutations of } (\omega_1',\omega_2') \text{ and } (\omega_1,\omega_2,\omega_3)]\\ &\quad+\frac{-\mathrm{i}\Gamma_{1D}^2\,(2\pi)^2\delta(\omega_2'+\omega_3'-\omega_2-\omega_3)\delta(\omega_1'-\omega_1)}{(\omega_2-\omega_0+\mathrm{i}\Gamma)(\omega_2-\omega_2'+\mathrm{i}0)(\omega_3'-\omega_0+\mathrm{i}\Gamma)}\\ &\quad+\text{ [permutations of } (\omega_1',\omega_2') \text{ and } (\omega_1,\omega_2,\omega_3)]\\ &\quad+s(\omega_3')(2\pi)^3\delta(\omega_1'-\omega_1)\delta(\omega_2'-\omega_2)\delta(\omega_3'-\omega_3)\\ &\quad+\text{ [permutations of } (\omega_1,\omega_2,\omega_3)].\end{aligned} \tag{C2}$$

Here, the first contributions stand for the irreducible part of the scattering amplitude, the second contributions reduce to the two-photon scattering and the other photon passing the system without interaction, and the third contributions correspond to single-photon scattering and the other two photons passing without interaction.

Performing Fourier transform over $\omega_1', \omega_2', \omega_3'$ we get

$$\begin{aligned} S^{XXXx\leftarrow XXXx}_{t_1,t_2,t_3\leftarrow\omega_1,\omega_2,\omega_3} &= s(\omega_1)s(\omega_2)s(\omega_3)\big(1-\mathrm{e}^{(\mathrm{i}\omega_2-\Gamma)(t_{(2)}-t_{(1)})}\big)\big(1-\mathrm{e}^{(\mathrm{i}\omega_3-\Gamma)(t_{(3)}-t_{(2)})}\big)\mathrm{e}^{-\mathrm{i}(\omega_1 t_{(1)}+\omega_2 t_{(2)}+\omega_3 t_{(3)})} \\ &+ s(\omega_1)s(\omega_2)\big(\mathrm{e}^{-\mathrm{i}\omega_1 t_{(1)}-\mathrm{i}\omega_2 t_{(2)}}-\mathrm{e}^{-\mathrm{i}\omega_1 t_{(1)}-\mathrm{i}\omega_2 t_{(1)}-\Gamma(t_{(2)}-t_{(1)})}\big)\mathrm{e}^{-\mathrm{i}\omega_3 t_{(3)}} \\ &+ s(\omega_2)s(\omega_3)(\mathrm{e}^{-\mathrm{i}\omega_2 t_{(2)}-\mathrm{i}\omega_3 t_{(3)}}-\mathrm{e}^{-\mathrm{i}\omega_2 t_{(2)}-\mathrm{i}\omega_3 t_{(2)}-\Gamma(t_{(3)}-t_{(2)})})\mathrm{e}^{-\mathrm{i}\omega_1 t_{(1)}} \\ &+ s(\omega_1)s(\omega_3)(\mathrm{e}^{-\mathrm{i}\omega_1 t_{(1)}-\mathrm{i}\omega_3 t_{(3)}}-\mathrm{e}^{-\mathrm{i}\omega_1 t_{(1)}-\mathrm{i}\omega_3 t_{(1)}-\Gamma(t_{(3)}-t_{(1)})})\mathrm{e}^{-\mathrm{i}\omega_2 t_{(2)}} \\ &+ [1+s(\omega_1)+s(\omega_2)+s(\omega_3)]\mathrm{e}^{-\mathrm{i}(\omega_1 t_{(1)}+\omega_2 t_{(2)}+\omega_3 t_{(3)})}+[\text{permutations of }(\omega_1,\omega_2,\omega_3)], \end{aligned} \tag{C3}$$

$$\begin{aligned} S^{XXYy\leftarrow XXXx}_{t_1,t_2,t_3\leftarrow\omega_1,\omega_2,\omega_3} &= \theta_{t_3-t_>}s(\omega_1)s(\omega_2)s(\omega_3)\big(1-\mathrm{e}^{(\mathrm{i}\omega_2-\Gamma)(t_{(2)}-t_{(1)})}\big)\big(1-\mathrm{e}^{(\mathrm{i}\omega_3-\Gamma)(t_{(3)}-t_{(2)})}\big)\mathrm{e}^{-\mathrm{i}(\omega_1 t_{(1)}+\omega_2 t_{(2)}+\omega_3 t_{(3)})} \\ &+ \theta_{t_3-t_>}s(\omega_2)s(\omega_3)\big(\mathrm{e}^{-\mathrm{i}\omega_2 t_>-\mathrm{i}\omega_3 t_3}-\mathrm{e}^{-\mathrm{i}\omega_2 t_>-\mathrm{i}\omega_3 t_>-\Gamma(t_3-t_>)}\big)\mathrm{e}^{-\mathrm{i}\omega_1 t_<} \\ &+ \theta_{t_3-t_<}s(\omega_1)s(\omega_3)\big(\mathrm{e}^{-\mathrm{i}\omega_1 t_<-\mathrm{i}\omega_3 t_3}-\mathrm{e}^{-\mathrm{i}\omega_1 t_<-\mathrm{i}\omega_3 t_<-\Gamma(t_3-t_<)}\big)\mathrm{e}^{-\mathrm{i}\omega_2 t_>} \\ &+ s(\omega_3)\mathrm{e}^{-\mathrm{i}(\omega_1 t_<+\omega_2 t_>+\omega_3 t_3}+[\text{permutations of }(\omega_1,\omega_2,\omega_3)]. \end{aligned} \tag{C4}$$

Here, $t_{(1)} \leqslant t_{(2)} \leqslant t_{(3)}$ are the sorted values of t_1, t_2, t_3, $t_< = \min(t_1, t_2)$, $t_> = \max(t_1, t_2)$.

APPENDIX D: *N*-PHOTON ENTANGLEMENT IN A QUASIMONOCHROMATIC APPROXIMATION

Here, we consider transmission of wide N-photon Gaussian pulses with $\gamma \to 0$ which are nearly monochromatic. Due to large temporal broadening of the pulse, the probability that two photons interact with the atom with a small delay $\lesssim 1/\Gamma$ is negligible. We suppose that $t_1 < t_2 < \ldots t_N$, and $|t_{n+1} - t_n| \gg \Gamma$, so the photons get transmitted one-by-one. Then, the transmitted pulse envelopes read

$$\psi^{X^N x}_{t_1\ldots t_N} = |t(\omega)|^{2N}\psi^{(0)}_{t_1}\ldots\psi^{(0)}_{t_N}, \tag{D1}$$

$$\psi^{X^{N-k}YX^{k-1}y}_{t_1\ldots t_N} = |t(\omega)|^{2(N-k)}|s(\omega)|^2\psi^{(0)}_{t_1}\ldots\psi^{(0)}_{t_N}, \tag{D2}$$

where $1 \leqslant k \leqslant N$. Then the probability to convert the state of the atom and N transmitted photons to the canonical W_{N+1}, averaged over the photon detection times $t_1 \ldots t_N$, is calculated as

$$\begin{aligned} \langle P_{W_{N+1}}\rangle_\omega &= (N+1)\int\ldots\int dt_1\ldots dt_N \\ &\times \min\big[\psi^{X^N x}_{t_1\ldots t_N}, \psi^{X^{N-1}Yy}_{t_1\ldots t_N}, \ldots, \psi^{YX^{N-1}y}_{t_1\ldots t_N}\big]. \end{aligned} \tag{D3}$$

Substituting here the expressions Eqs. (D1) and (D2) we finally obtain

$$\langle P_{W_{N+1}}\rangle_\omega = (N+1)|t(\omega)|^{2(N-1)}\min[|t(\omega)|^2, |s(\omega)|^2]. \tag{D4}$$

For $N \geqslant 2$ the maximum of $\langle P_{W_{N+1}}\rangle_\omega$ is achieved at

$$\omega_{\max} = \omega_0 \pm \sqrt{(N-1)\Gamma^2 - N\Gamma'^2} \tag{D5}$$

and reads

$$\big\langle P_{W_{N+1}}\big\rangle_{\omega_{\max}} = \frac{\Gamma_{1D}}{\Gamma_{1D}+2\Gamma'}\frac{N+1}{N-1}\left(1-\frac{1}{N}\right)^N. \tag{D6}$$

Interestingly, the probability $\langle P_{W_{N+1}}\rangle_{\omega_{\max}}$ has a nonzero limit when the number of input photons is increased, $N \to \infty$, i.e.,

$$\langle P_{W_\infty}\rangle_{\omega_{\max}} \to \frac{\Gamma_{1D}}{\Gamma_{1D}+2\Gamma'}\frac{1}{\mathrm{e}}. \tag{D7}$$

Even in the presence of losses, $\Gamma' \neq 0$, the probability $\langle P_{W_{N+1}}\rangle_{\omega_{\max}}$ remains finite. The conditional probability to convert the system state into W_{N+1} state, given none of the photons are lost upon transmission, is even higher. It can be calculated as $\langle P_{W_{N+1}}\rangle/T_N$, where T_N is the N-photon transmission probability. For the quasi-monochromatic pulse the latter reads

$$T_N(\omega) = |t(\omega)|^{2N} + |s(\omega)|^2\frac{1-|t(\omega)|^{2N}}{1-|t(\omega)|^2}. \tag{D8}$$

Then the conditional probability assumes the form

$$\frac{\big\langle P_{W_{N+1}}\big\rangle_{\omega_{\max}}}{T_N(\omega_{\max})} = \frac{(N+1)/(N-1)}{(1-1/N)^{-N}+2\Gamma'/\Gamma_{1D}} \tag{D9}$$

and at $N \to \infty$ tends to $1/(\mathrm{e}+2\Gamma'/\Gamma_{1D})$.

APPENDIX E: PULSE SHAPE OPTIMIZATION

To maximize the entanglement of the scattered photons, we perform an optimization of the incident pulse shape. Namely, we take

$$\varphi^{(0)}_t = \left[1+\sum_{n=2}^{\infty}(a_n+\mathrm{i}b_n)H_n(\gamma t)\right]\mathrm{e}^{-\mathrm{i}\omega t-\gamma^2 t^2/2}, \tag{E1}$$

where a_n (for $n = 3, 4, \ldots$) and b_n (for $n = 2, 3, 4, \ldots$) are the new free parameters. We fix $a_1 = b_1 = a_2 = 0$. They would correspond to a variation of the pulse arrival time (that does not affect transmission), central frequency, and width (that we vary using the parameters ω and γ). We substitute the pulse Eq. (E1) into Eqs. (8) and (15) and (16) to calculate the transmitted pulse.

Finally, the values of $\langle P_{W_{3,4}}\rangle$ are calculated numerically and maximized using the conjugate gradient method. The results are given in Table I.

APPENDIX F: ONE-PHOTON TRANSMISSION THROUGH AN ARRAY OF Λ ATOMS

Here, we consider transmission of a quasimonochromatic one-photon pulse $\gamma \to 0$, through an array of M Λ-atoms. The incident photon is assumed to be X polarized, while all the atoms are initially in the x state. Upon the transmission,

TABLE I. The amplitudes of the higher-order temporal harmonics of the envelopes for incident two- and three-photon pulse that correspond to the maximal values of $\langle P_{W_3}\rangle$ and $\langle P_{W_4}\rangle$ in the absence of loss $\Gamma' = 0$.

	$\langle P_{W_3}\rangle$ 0.8018	$\langle P_{W_4}\rangle$ 0.6237
ω/Γ_{1D}	0.8984	0.6747
γ/Γ_{1D}	1.0143	1.2721
b_2	0.0294	0.0373
a_3	0.0062	0.0021
b_3	0.0147	0.0130
a_4	0.0024	0.0050

at most one atom can switch to the y state, and the photon then flips its polarization. We consider here a chiral setup, where the photons can propagate in one direction only. Then, the scattering matrix of the system is given by the product of M scattering matrices of the individual atoms. For a quasi-monochromatic single-photon pulse with frequency ω, the transmission amplitudes read

$$\psi_t^{Xx^M} = t^N(\omega)\psi_t^{(0)}, \tag{F1}$$

$$\psi_t^{Yx^{M-k}yx^{k-1}} = t^{M-k}(\omega)s^k(\omega)\psi_t^{(0)}, \tag{F2}$$

where $1 \leqslant k \leqslant M$. The final state is an entangled state of the transmitted photon and all the atoms. The probability to convert it to the canonical W_{M+1} state is given by the same expressions as for the case of one atom and M photons, see Eqs. (D4) to (D7).

[1] O. Gühne and G. Tóth, Entanglement detection, Phys. Rep. **474**, 1 (2009).

[2] R. Horodecki, P. Horodecki, M. Horodecki, and K. Horodecki, Quantum entanglement, Rev. Mod. Phys. **81**, 865 (2009).

[3] A. Karlsson and M. Bourennane, Quantum teleportation using three-particle entanglement, Phys. Rev. A **58**, 4394 (1998).

[4] W. Dür, G. Vidal, and J. I. Cirac, Three qubits can be entangled in two inequivalent ways, Phys. Rev. A **62**, 062314 (2000).

[5] P. Agrawal and A. Pati, Perfect teleportation and superdense coding with W states, Phys. Rev. A **74**, 062320 (2006).

[6] H. J. Briegel and R. Raussendorf, Persistent entanglement in arrays of interacting particles, Phys. Rev. Lett. **86**, 910 (2001).

[7] R. Raussendorf and H. J. Briegel, A one-way quantum computer, Phys. Rev. Lett. **86**, 5188 (2001).

[8] E. Knill, R. Laflamme, and G. J. Milburn, A scheme for efficient quantum computation with linear optics, Nature (London) **409**, 46 (2001).

[9] D. Roy, C. M. Wilson, and O. Firstenberg, *Colloquium*: Strongly interacting photons in one-dimensional continuum, Rev. Mod. Phys. **89**, 021001 (2017).

[10] D. E. Chang, J. S. Douglas, A. González-Tudela, C.-L. Hung, and H. J. Kimble, *Colloquium:* Quantum matter built from nanoscopic lattices of atoms and photons, Rev. Mod. Phys. **90**, 031002 (2018).

[11] A. S. Sheremet, M. I. Petrov, I. V. Iorsh, A. V. Poshakinskiy, and A. N. Poddubny, Waveguide quantum electrodynamics: Collective radiance and photon-photon correlations, Rev. Mod. Phys. **95**, 015002 (2023).

[12] T. C. Ralph, I. Söllner, S. Mahmoodian, A. G. White, and P. Lodahl, Photon sorting, efficient Bell measurements, and a deterministic controlled-Z gate using a passive two-level nonlinearity, Phys. Rev. Lett. **114**, 173603 (2015).

[13] D. Ilin, A. V. Poshakinskiy, A. N. Poddubny, and I. Iorsh, Frequency combs with parity-protected cross-correlations and entanglement from dynamically modulated qubit arrays, Phys. Rev. Lett. **130**, 023601 (2023).

[14] D. Pinotsi and A. Imamoglu, Single photon absorption by a single quantum emitter, Phys. Rev. Lett. **100**, 093603 (2008).

[15] S. Rosenblum, O. Bechler, I. Shomroni, Y. Lovsky, G. Guendelman, and B. Dayan, Extraction of a single photon from an optical pulse, Nat. Photon. **10**, 19 (2016).

[16] K. Koshino, S. Ishizaka, and Y. Nakamura, Deterministic photon-photon $\sqrt{\text{SWAP}}$ gate using a Λ system, Phys. Rev. A **82**, 010301(R) (2010).

[17] S. Rosenblum, A. Borne, and B. Dayan, Analysis of deterministic swapping of photonic and atomic states through single-photon Raman interaction, Phys. Rev. A **95**, 033814 (2017).

[18] O. Bechler, A. Borne, S. Rosenblum, G. Guendelman, O.E. Mor, M. Netser, T. Ohana, Z. Aqua, N. Drucker, R. Finkelstein, Y. Lovsky, R. Bruch, D. Gurovich, E. Shafir, and B. Dayan, A passive photon–atom qubit swap operation, Nat. Phys. **14**, 996 (2018).

[19] Z. Aqua, M. S. Kim, and B. Dayan, Generation of optical Fock and W states with single-atom-based bright quantum scissors, Photon. Res. **7**, A45 (2019).

[20] N. H. Lindner and T. Rudolph, Proposal for pulsed on-demand sources of photonic cluster state strings, Phys. Rev. Lett. **103**, 113602 (2009).

[21] I. Schwartz, D. Cogan, E. R. Schmidgall, Y. Don, L. Gantz, O. Kenneth, N. H. Lindner, and D. Gershoni, Deterministic generation of a cluster state of entangled photons, Science **354**, 434 (2016).

[22] D. Istrati, Y. Pilnyak, J. C. Loredo, C. Antón, N. Somaschi, P. Hilaire, H. Ollivier, M. Esmann, L. Cohen, L. Vidro, C. Millet, A. Lemaître, I. Sagnes, A. Harouri, L. Lanco, P. Senellart, and H. S. Eisenberg, Sequential generation of linear cluster states from a single photon emitter, Nat. Commun. **11**, 5501 (2020).

[23] D. S. Smirnov, B. Reznychenko, A. Auffèves, and L. Lanco, Measurement back action and spin noise spectroscopy in a charged cavity QED device in the strong coupling regime, Phys. Rev. B **96**, 165308 (2017).

[24] H. Pichler, S. Choi, P. Zoller, and M. D. Lukin, Universal photonic quantum computation via time-delayed feedback, Proc. Natl. Acad. Sci. USA **114**, 11362 (2017).

[25] P. Thomas, L. Ruscio, O. Morin, and G. Rempe, Efficient generation of entangled multiphoton graph states from a single atom, Nature (London) **608**, 677 (2022).

[26] V. I. Rupasov and V. I. Yudson, Exact Dicke superradiance theory: Bethe wavefunctions in the discrete atom model, Sov. Phys. JETP **59**, 478 (1984).

[27] J.-T. Shen and S. Fan, Strongly correlated two-photon transport in a one-dimensional waveguide coupled to a two-level system, Phys. Rev. Lett. **98**, 153003 (2007).

[28] T. Shi and C. P. Sun, Lehmann-Symanzik-Zimmermann reduction approach to multiphoton scattering in coupled-resonator arrays, Phys. Rev. B **79**, 205111 (2009).

[29] H. Zheng and H. U. Baranger, Persistent quantum beats and long-distance entanglement from waveguide-mediated interactions, Phys. Rev. Lett. **110**, 113601 (2013).

[30] S. Xu and S. Fan, Input-output formalism for few-photon transport: A systematic treatment beyond two photons, Phys. Rev. A **91**, 043845 (2015).

[31] R. Trivedi, K. Fischer, S. Xu, S. Fan, and J. Vuckovic, Few-photon scattering and emission from low-dimensional quantum systems, Phys. Rev. B **98**, 144112 (2018).

[32] T. Shi, D. E. Chang, and J. I. Cirac, Multiphoton-scattering theory and generalized master equations, Phys. Rev. A **92**, 053834 (2015).

[33] A. González-Tudela, V. Paulisch, D. E. Chang, H. J. Kimble, and J. I. Cirac, Deterministic generation of arbitrary photonic states assisted by dissipation, Phys. Rev. Lett. **115**, 163603 (2015).

[34] T. Caneva, M. T. Manzoni, T. Shi, J. S. Douglas, J. I. Cirac, and D. E. Chang, Quantum dynamics of propagating photons with strong interactions: A generalized input–output formalism, New J. Phys. **17**, 113001 (2015).

[35] Y. L. Fang and H. U. Baranger, Photon correlations generated by inelastic scattering in a one-dimensional waveguide coupled to three-level systems, Physica E **78**, 92 (2016).

[36] O. A. Iversen and T. Pohl, Strongly correlated states of light and repulsive photons in chiral chains of three-level quantum emitters, Phys. Rev. Lett. **126**, 083605 (2021).

[37] D. Witthaut and A. S. Sørensen, Photon scattering by a three-level emitter in a one-dimensional waveguide, New J. Phys. **12**, 043052 (2010).

[38] Y. Li, L. Aolita, Darrick E. Chang, and L. C. Kwek, Robust-fidelity atom-photon entangling gates in the weak-coupling regime, Phys. Rev. Lett. **109**, 160504 (2012).

[39] M. Bradford and J.-T. Shen, Single-photon frequency conversion by exploiting quantum interference, Phys. Rev. A **85**, 043814 (2012).

[40] C. Martens, P. Longo, and K. Busch, Photon transport in one-dimensional systems coupled to three-level quantum impurities, New J. Phys. **15**, 083019 (2013).

[41] S. Das, V. E. Elfving, F. Reiter, and A. S. Sørensen, Photon scattering from a system of multilevel quantum emitters. II. Application to emitters coupled to a one-dimensional waveguide, Phys. Rev. A **97**, 043838 (2018).

[42] J. Zhong, Rituraj, F. Dinc, and S. Fan, Detecting the relative phase between different frequency components of a photon using a three-level Λ atom coupled to a waveguide, Phys. Rev. A **107**, L051702 (2023).

[43] Z. L. Zhang and L.-P. Yang, Limits of single-photon storage in a single Λ-type atom, Phys. Rev. A **107**, 063704 (2023).

[44] M. L. Chan, A. Tiranov, M. H. Appel, Y. Wang, L. Midolo, S. Scholz, A. D. Wieck, A. Ludwig, A. S. Sørensen, and P. Lodahl, On-chip spin-photon entanglement based on photon-scattering of a quantum dot, npj Quantum Inf. **9**, 49 (2023).

[45] A. N. Poddubny, S. Rosenblum, and B. Dayan, How single-photon nonlinearity is quenched with multiple quantum emitters: Quantum Zeno effect in collective interactions with Λ-level atoms, arXiv:2401.06997.

[46] M. Yang and Z. L. Cao, Entanglement distillation for *W* class states, Physica A **337**, 141 (2004).

[47] L. Scarpelli, B. Lang, F. Masia, D. M. Beggs, E. A. Muljarov, A. B. Young, R. Oulton, M. Kamp, S. Höfling, C. Schneider, and W. Langbein, 99% beta factor and directional coupling of quantum dots to fast light in photonic crystal waveguides determined by spectral imaging, Phys. Rev. B **100**, 035311 (2019).

[48] M. Mirhosseini, E. Kim, X. Zhang, A. Sipahigil, P. B. Dieterle, A. J. Keller, A. Asenjo-Garcia, D. E. Chang, and O. Painter, Cavity quantum electrodynamics with atom-like mirrors, Nature (London) **569**, 692 (2019).

[49] A. M. Vadiraj, Andreas Ask, T. G. McConkey, I. Nsanzineza, C. W. Sandbo Chang, A. F. Kockum, and C. M. Wilson, Engineering the level structure of a giant artificial atom in waveguide quantum electrodynamics, Phys. Rev. A **103**, 023710 (2021).